

Supporting Information of

Enhanced performance and Light Soaking Stability of Planar Perovskite Solar Cells using Amine-based Fullerene Interfacial Modifier

Yunhai Zhang^{a,b}, Peng Wang^b, Xuegong Yu^{a,}, Jiangsheng Xie^a, Jiabin Huang^a, Lingbo Xu^b, Can Cui^{b,*}, Ming Lei^{c,*} and Deren Yang^a*

(a) State Key Lab of Silicon Materials and School of Materials Science & Engineering, Zhejiang University, Hangzhou 310027, China

(b) Center for Optoelectronics Materials and Devices, Department of Physics, Zhejiang Sci-Tech University, Hangzhou 310018, China

(c) Department of Chemistry, Zhejiang University, Hangzhou, Zhejiang 310027, China

*Corresponding author:

Xuegong Yu Email: yuxuegong@zju.edu.cn

Can Cui Email: cancui@zstu.edu.cn

Ming Lei Email: leiming@zju.edu.cn

Table of contents:

Figure S1. To-view SEM images of electron transport layers without and with PCBDNA modification. (a) FTO/TiO₂; (b) FTO/TiO₂/PCBDAN.

Figure S2. Tapping-mode AFM images.

Figure S3. The images of DMF droplet angles.

Figure S4. Photovoltaic performance statistics of the devices.

Figure S5. J-V curves under different decay times and the corresponding parameters.

Figure S6. The steady-state J_{sc} test at the voltage around 0.732 V of the control device.

Figure S7. The normalized absorption intensity of perovskite films based on Glass and Glass/PCBDAN at 600 nm.

Figure S8. Device efficiency stability under sustained AM1.5G illumination soaking with encapsulation in air condition.

Table S1. Work function (WF) of FTO, TiO₂ and TiO₂/PCBDAN from Kelvin probe force microscopy (KPFM).

Table S2. The TRPL fitting characteristics of perovskite thin films on TiO₂ and TiO₂/PCBDNAN ETL.

Table S3. Photovoltaic parameters of PSCs with different delay times.

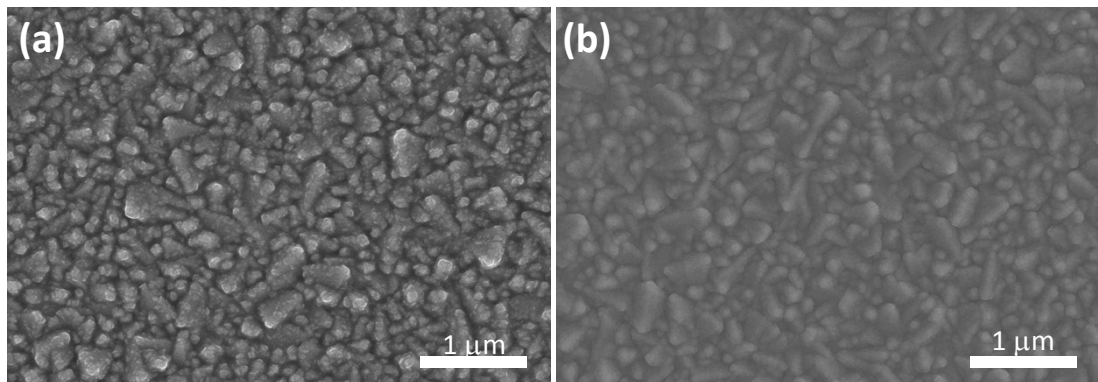


Figure S1. To-view SEM images of electron transport layers without and with PCBDNA modification. (a) FTO/TiO₂; (b) FTO/TiO₂/PCBDAN.

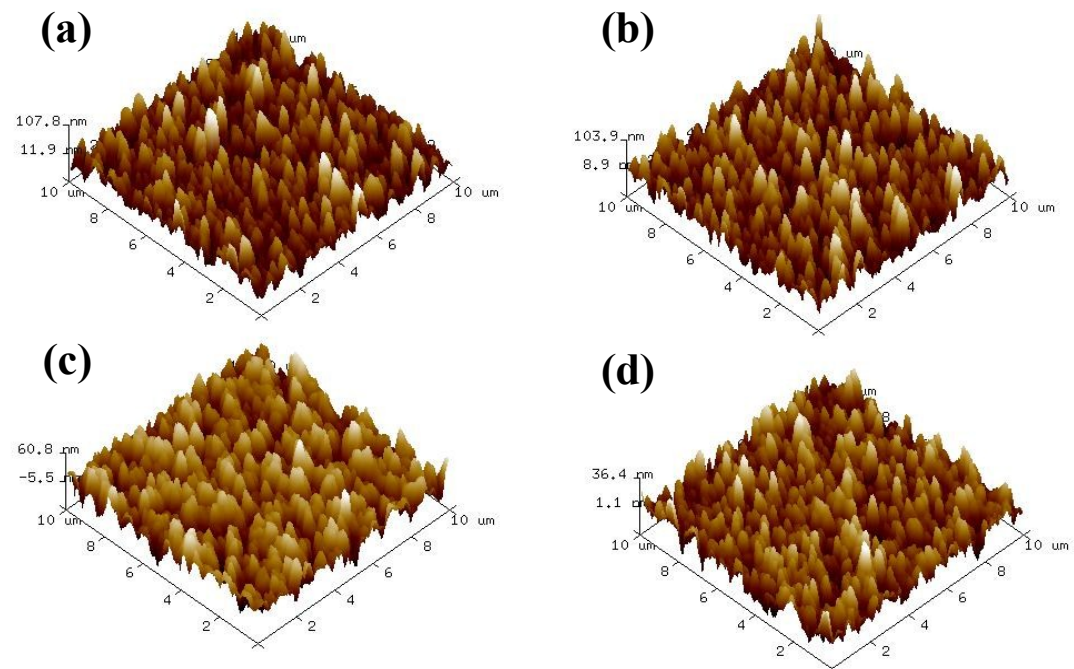


Figure S2. Tapping-mode AFM images of ETLs and perovskites with and without PCBDAN (a) FTO/TiO₂, (b) FTO/TiO₂/PCBDAN, (c) FTO/TiO₂/Perovskite and (d) FTO/TiO₂/PCBDAN/Perovskite. The RMS roughness values for the images of a-d are 27.7 nm, 27.0 nm, 18.9 nm and 9.9 nm, respectively.

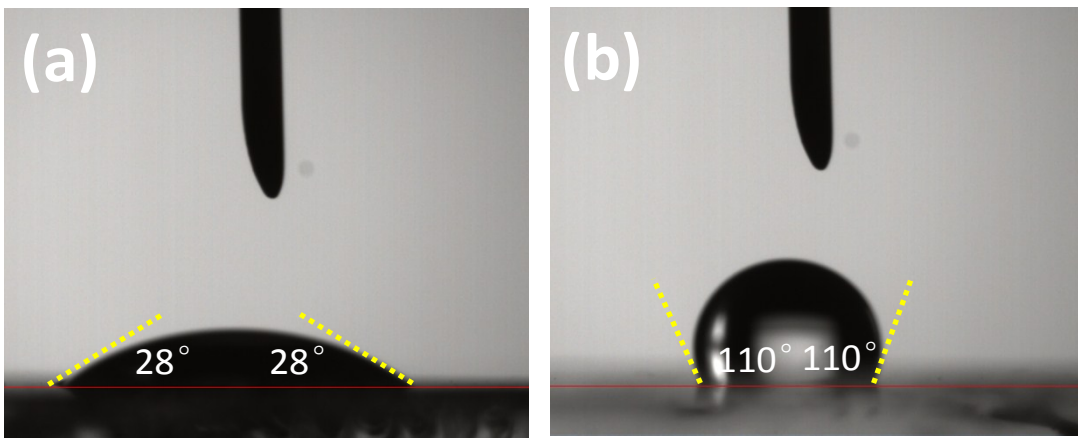


Figure S3. The images of DMF droplet angle on TiO_2 ETL without and with PCBDAN modification. (a) without PCBDAN (b) with PCBDAN.

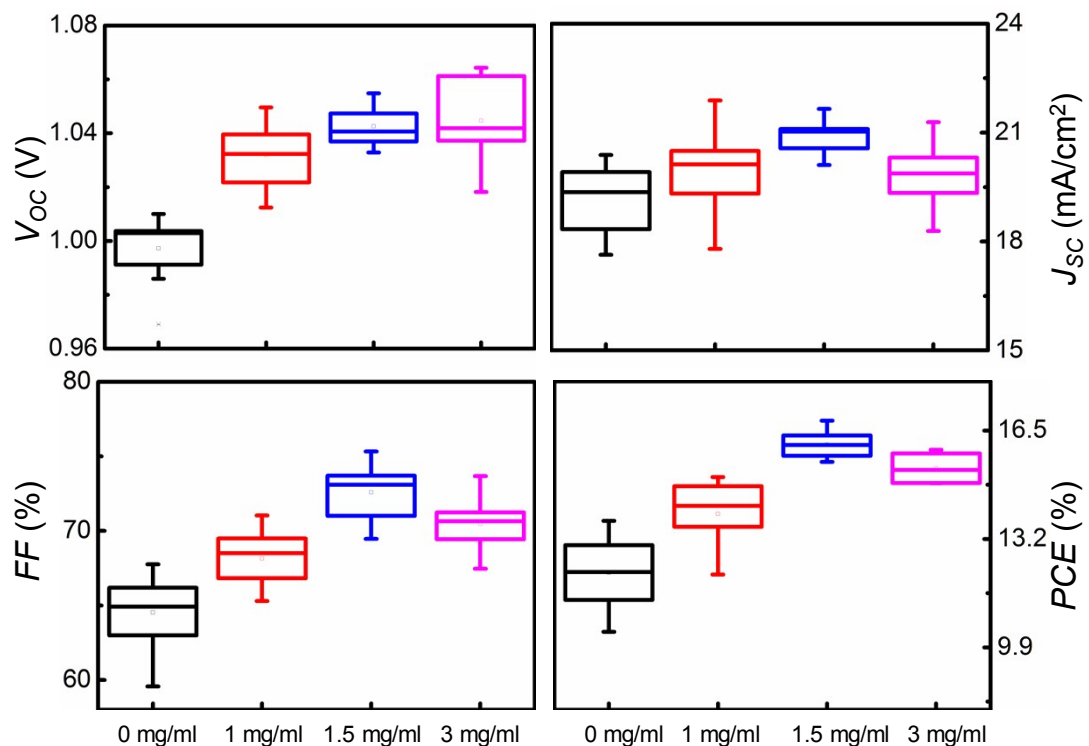


Figure S4. Photovoltaic performance statistics of the devices with different concentration of PCBDAN under 100 mW/cm^2 illumination, in which data are extracted from their J - V characteristics.

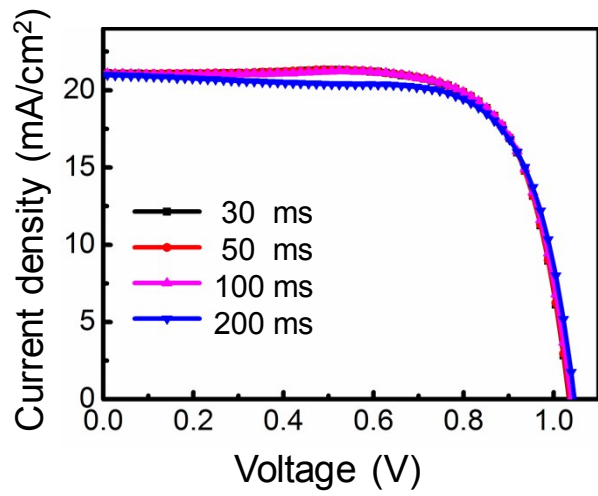


Figure S5. J-V curves under different decay times.

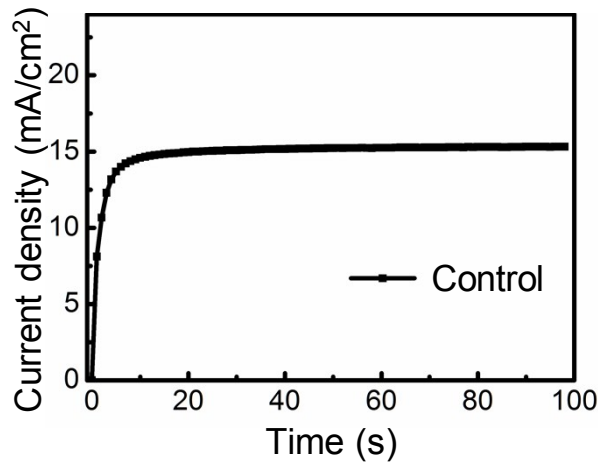


Figure S6. The steady-state J_{sc} test at the voltage around 0.785 V of the control device.

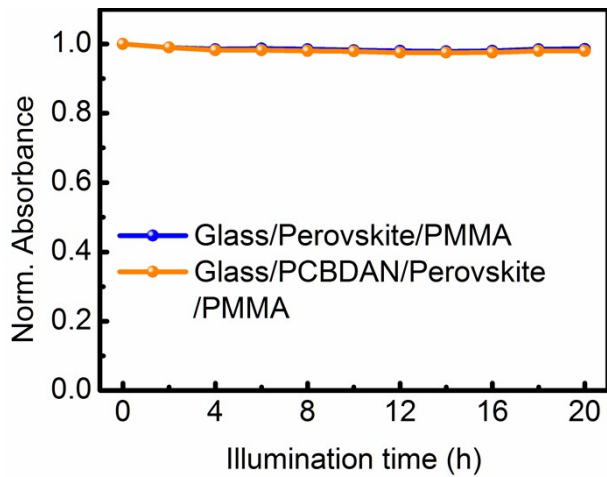


Figure S7. The normalized absorption intensity of perovskite films based on Glass and Glass/PCBDAN at 600 nm.

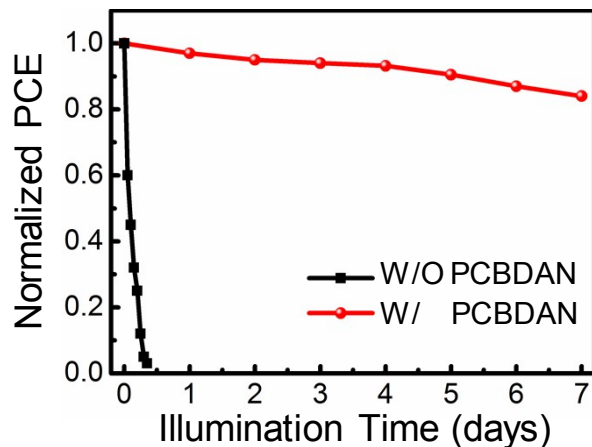


Figure S8. Device efficiency stability under sustained AM1.5G illumination soaking with encapsulation in air condition.

Table S1. Work function (WF) of FTO, TiO₂ and TiO₂/PCBDAN from Kelvin probe force microscopy (KPFM).

	FTO	FTO/TiO ₂	FTO/TiO ₂ /PCBDA N
Relative values (mV)	224	133	-146.9
Work function (V)	4.300	4.209	3.930

Table S2. TRPL fitting characteristics of perovskite thin films on TiO₂ and TiO₂/PCBDAN ETL.

ETL	A ₁	τ ₁ (ns)	A ₂	τ ₂ (ns)	Average τ((ns)
W/O PCBDAN	0.267	3.12	0.56	34.3	24.2
W/ PCBDAN	0.19	1.76	0.75	21.96	17.9

Table S3. Photovoltaic parameters of PSCs with different delay times.

Decay time (ms)	V _{OC} (V)	J _{SC} (mA/cm ²)	FF (%)	PCE (%)
30	1.0342	21.086	73.62	16.05
50	1.0353	21.095	73.54	16.06
100	1.0393	21.097	73.27	16.06
200	1.0463	20.993	71.62	15.73